

# Cavity-enabled self-electro-optic bistability in silicon photonics

Arka Majumdar<sup>1,\*</sup> and Armand Rundquist<sup>2</sup>

<sup>1</sup>Electrical Engineering, University of Washington, Seattle, Washington 98195, USA

<sup>2</sup>E. L. Ginzton Laboratory, Stanford University, Stanford, California 94305, USA

\*Corresponding author: arka@uw.edu

Received April 24, 2014; revised May 21, 2014; accepted May 24, 2014;  
posted May 27, 2014 (Doc. ID 210386); published June 24, 2014

We propose a new type of bistable device for silicon photonics, using the self-electro-optic effect within an optical cavity. Since the bistability does not depend on the intrinsic optical nonlinearity of the material, but is instead engineered by means of optoelectronic feedback, it appears at low optical powers. This bistable device satisfies all the basic criteria required in an optical switch to build a scalable digital optical computing system. © 2014 Optical Society of America

OCIS codes: (130.4815) Optical switching devices; (200.4660) Optical logic; (230.1150) All-optical devices.  
<http://dx.doi.org/10.1364/OL.39.003864>

Significant progress in silicon photonics in the last decade has helped to bring the long-standing goal of optical interconnects closer to reality. With several large companies working on developing optical interconnects for data centers, we can surmise that in the near future such optical interconnects will proliferate throughout the computing sphere. At that point, the excess latency and energy consumption incurred in electro-optic signal conversions will be increasingly prohibitive, and so it will become necessary to perform computations directly on the optical signal. Hence, in the very near future, even though optical computing will not be a competitive technology to the existing digital computers for all applications, an increase in optical interconnects will necessitate such optical computing for specific tasks.

In general, a digital computer requires two stable states to code one bit of information, which can be achieved by exploiting optical bistability [1]. However, a simple demonstration of optical bistability is not sufficient for building an optical computing system. In fact, several approaches to optical computing have been reported in the literature, but few of them satisfy all the basic criteria that are essential to build a scalable and useful digital computing system [2]. One of the few successful approaches is an optical switch based on the self-electro-optic (SEO) bistable effect [3]. In an SEO effect device, one engineers positive optoelectronic feedback by using a photodetector and an electro-optic modulator, which together generate optical bistability. The development of optical interconnects will require the perfection of electro-optic modulators and photodetectors, which are precisely the components necessary to build a high-performance SEO effect device. Thus we can expect that, as the technology for building optical interconnects improves, such gains will also be realized in the quality of SEO effect devices. Additionally, a system based on SEO effect devices provides homogeneous architecture, as the basic components of the computing device can also be used independently as modulators and detectors, greatly simplifying the task of system integration.

Previous SEO effect devices, however, were primarily based on quantum confined Stark effects (QCSE) in

quantum wells fabricated in III–V materials. The switching energy of these devices was on the order of hundreds of picojoules, which is much larger than an electronic switch [3]. Additionally, building a system out of III–V materials also presents a challenge. In the current work, we analyze the possibility of realizing such effects in silicon photonics, which is potentially a much more scalable platform. With silicon photonics going fabless [4], there is great opportunity for innovation in designing and building a large-scale integrated optical system. Although a straightforward approach would be to use a Si–Ge quantum well and the resulting QCSE [5], the growth of this material system is complicated. Here, we propose a way to obtain the SEO effect in the silicon photonics platform using ring cavities (embedded in a p–i–n diode) with an integrated photodetector. The photodetector can be realized either by doping a specific region in the ring and using defect-mediated sub-bandgap photodetection [6] or by depositing a layer of absorbing material on silicon, such as graphene [7] or III–V materials [8]. With the incorporation of a high-quality factor cavity, the switching energy can also be greatly reduced.

Let us first analyze a generic optically bistable system based on a cavity [Fig. 1(a)]. The dynamics of a cavity driven by an external laser can be described by the equation:

$$\frac{da(t)}{dt} = i\Delta a(t) - [\gamma_c + \gamma_l]a(t) + i\sqrt{2\gamma_c}S_{in},$$

where  $a(t)$  denotes the intracavity field,  $\Delta$  is the detuning of the laser from the cavity resonance,  $\gamma_c$  is the coupling rate of the cavity to the outside channel,  $\gamma_l$  is the loss in the cavity, and  $S_{in}$  denotes the amplitude of the input light field. The output field is given by  $S_{out} = S_{in} + i\sqrt{2\gamma_c}a$ . In the steady state, the input, output, and absorbed power are, respectively,  $P_{in} = |S_{in}|^2$ ,  $P_{out} = ((\gamma_c - \gamma_l)^2 + \Delta^2)/(\gamma_c + \gamma_l)^2 + \Delta^2 P_{in}$ , and  $P_{abs} = (4\gamma_c\gamma_l)/(\gamma_c + \gamma_l)^2 + \Delta^2 P_{in}$ . We note that this dynamic model is very similar to the usual steady-state model of the ring [9] close to a resonance. A feedback loop in this system can be realized by shifting the cavity resonance in response to the absorbed power, the simplest

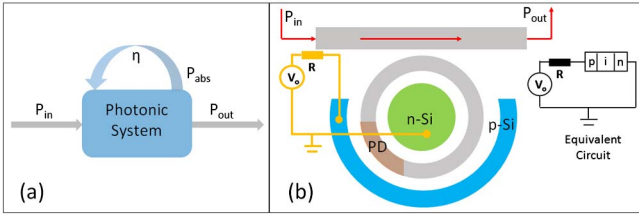


Fig. 1. (a) Block diagram for a generic optically bistable device. The bistability is caused by positive feedback. (b) Schematic of an SEO bistable device, conceived in a silicon photonics platform: a ring cavity in a p-i-n diode with an embedded photodetector (PD).

relation being  $\Delta = \Delta_o + \eta P_{\text{abs}}$ . Then the steady state of the device is governed by

$$\eta^2 P_{\text{abs}}^3 + 2\eta \Delta_o P_{\text{abs}}^2 + [(\gamma_c + \gamma_l)^2 + \Delta_o^2] P_{\text{abs}} = 4\gamma_c \gamma_l P_{\text{in}}.$$

This equation shows bistable behavior in the output power as a function of the input power, as long as  $\eta \Delta_o < 0$ , which causes the detuning of the cavity from the laser to change sign due to the feedback. In most optical bistabilities reported in silicon, this feedback is provided by two-photon absorption and the subsequent free carrier dispersion [10] or via a thermo-optic mechanism [11]. Significant progress has also been made in the bistability of a III-V nanocavity, based on electroabsorption and the free carrier effect [12–14]. However, all of these mechanisms provide little control to the user and, in general, require high optical powers. We also note that the optical power required to observe the bistability is inversely proportional to  $\eta$ , and, by changing  $\eta$ , one can change that power by orders of magnitude. By contrast, this optical power is not strongly dependent on the other parameters, such as the detuning or cavity losses.

In the SEO effect, we use an explicit opto-electronic feedback method to allow the absorbed power to change the cavity resonance, which provides the user with the ability to control the strength of the feedback. This method also does not depend on the intrinsic material optical nonlinearity, which is weak in silicon, and so our method has the potential to greatly reduce the optical power required to observe bistability. To implement the SEO effect, we propose to use a ring resonator fabricated in the intrinsic region of a p-i-n diode [Fig. 1(b)]. This is the most common configuration for a ring-based electro-optic modulator [15,16]. In this ring, we can create a photodetector region by any of the methods mentioned earlier.

For simplicity, we assume that the ring does not have any radiative loss and that most of the loss is coming from the absorption in the PD. The absorbed power in the PD gives rise to a photocurrent  $I_{\text{ph}} = SP_{\text{abs}}$ , with  $S$  being a constant. This current causes a change in the voltage  $V = V_o - RSP_{\text{abs}}$  across the cavity, shifting the cavity resonance. For a linear change in the cavity resonance with voltage, we can establish a one-to-one correspondence with the generic bistability. In practice, however, in a reverse-biased p-i-n junction, the applied voltage will cause a change in the width  $W_D$  of the depletion region as  $W_D \propto (V + V_{\text{bi}})^{1/2}$ ,  $V_{\text{bi}}$  being the built-in potential. This results in an effective change of the carrier concentration

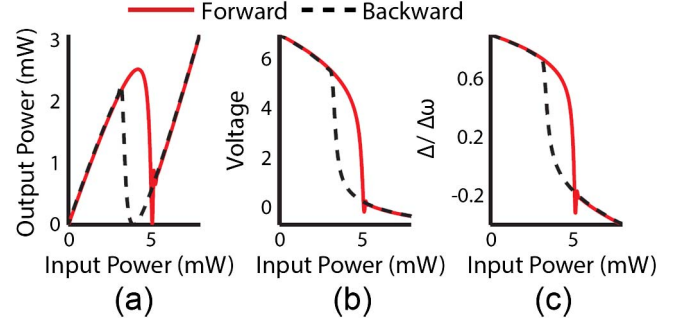


Fig. 2. (a) Cavity output power as a function of the input laser power for an SEO device, where the cavity modulation is achieved via the depletion capacitance of the diode, causing the cavity resonance to shift as a square root of the applied voltage. The parameters of the simulation are  $\Delta_o/2\pi = 200$  GHz,  $\gamma_c/2\pi = 10$  GHz and  $\gamma_l/2\pi = 10$  GHz,  $V_o = 7$  V,  $\alpha = 150$ ,  $R = 1.5$  k $\Omega$  and  $S = 1$  A/W. (b) The voltage across the diode and (c) the ring resonance shift  $\Delta$  normalized by the cavity linewidth  $\Delta\omega/2\pi \sim 200$  GHz, both as functions of the input power.

$\Delta n$  over a distance  $W_D$ , which in turn changes the refractive index [15] as  $\Delta n \propto \Delta N$ . The cavity resonance shift is linearly proportional to the change in the refractive index and can be written as

$$\Delta - \Delta_o \propto \Delta n \propto \alpha \sqrt{V_o - RSP_{\text{abs}} + V_{\text{bi}}},$$

where  $\alpha$  is a proportionality constant that depends on the particular nanophotonic cavity parameters; more specifically, the overlap of the cavity-confined electromagnetic field with the area where the carriers are changing. Figure 2 shows the results of numerical simulations under the realistic condition of carrier modulation by changes to the depletion width. We clearly observe optical bistability as a function of the input power. Note that in the simulation we assumed  $S = 1$  A/W, which is a rather large responsivity but is achievable with a graphene-based photodetector [17]. The sensitivity can also be increased by using a transimpedance amplifier. Moreover, we can compensate for a small  $S$  by using a large resistance  $R$ , but that will limit the speed. We note that the cavity resonance has to change by  $\sim 1$  nm to observe the bistability. Although such shifts are larger than the tuning ( $\sim 0.2$  nm) achievable with current silicon photonic modulators [16,18], their performance can be improved by increasing their phase efficiency. The tuning range can also be lowered at the cost of reduction of power output from the cavity. While the SEO bistability fundamentally depends on positive feedback, similarly engineered negative feedback, on the other hand, can be used to stabilize the ring resonators against thermal fluctuations [19].

Although the optical bistability arises from the SEO effect, useful optical computing requires a slightly more complicated device known as a “symmetric” SEO bistable device. In this arrangement, we use two SEO effect devices connected electrically in series [Fig. 3(a)]. Each of the devices acts as the load for the other, which can be controlled through exposure to light. In a symmetric SEO effect device, the operating point of the device depends on the amount of light incident on the two diodes. The current–voltage relation for the two diodes is given by

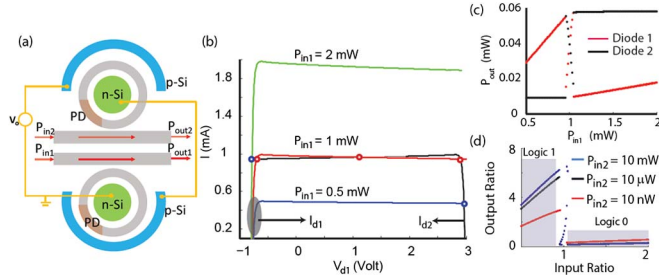


Fig. 3. (a) Schematic of a symmetric SEO bistable device, with two ring resonators connected electrically in series. (b) The current through diode 1 ( $I_{d1}$ ) and diode 2 ( $I_{d2}$ ) as a function of the voltage  $V_{d1}$  across diode 1 for different optical powers incident on diode 1 ( $P_{in1}$ ), but with the power incident on diode 2 fixed at  $P_{in2} = 1$  mW. The intersections of the two curves give the operating points. We note that, depending on the ratio of the input powers of the two diodes, we can have one or three points of operation. This gives rise to the bistability. (c) Output power  $P_{out}$  from the two ring cavities as a function of  $P_{in1}$  with  $P_{in2} = 1$  mW. (d) The bistable operation solely depends on the power ratio, showing that it can be used to achieve time-sequential gain. The logic 1 and logic 0 regions are highlighted.

$$I_{d1,2} = I_o e^{-q(V_{d1,2} + V_{bi})/kT} + I_{ph1,2}$$

where  $I_{d1,2}$  and  $V_{d1,2}$  are, respectively, the current and voltage across the two diodes, and  $I_{ph1,2}$  is the photocurrent in the diodes induced by the incident light on each of them ( $P_{in1,2}$ ). The operating point is given by the intersection of the I-V curves for the two diodes [Fig. 3(b)]. When the power incident on each diode is different (a ratio of 1:2 for the optical power will suffice), then the two curves intersect only at a single point [shown by the blue circles in Fig. 3(b)]. This shows that, depending on the ratio of input power each diode receives, most of the voltage will drop across one diode or the other. We note that when the ratio is equal (1:1), then there are three operating points (shown by the red circles). The center point of operation, where the voltage is equally distributed between the two diodes, is an unstable one, which will be crossed when the optical power incident on one diode changes from a low to high value. However, if the amount of optical power is very low, the generated photocurrent is negligible, causing an equal voltage drop across both diodes. This will ultimately decide the lowest power at which the switch can work. Figure 3(c) shows the output powers from the two rings as a function of the input optical power incident on diode 1 ( $P_{in1}$ ), with the incident optical power on diode 2 kept constant at 1 mW. Clear bistable behavior is observed in the output power from both diodes.

A symmetric SEO effect device satisfies all the basic criteria [2] of an optical switch required to perform digital optical computing. First, we use a single polarization and frequency of light, so, several devices can be cascaded without any additional overhead. Also, due to the bistability, the signal is cleaned in every stage, preventing noise in the signal from propagating through the system. Most optical switches based on an optical bistability satisfy these two criteria. However, these devices fail to satisfy other criteria, such as control-to-signal isolation and robustness to input power fluctuation.

The fundamentally different property of a symmetric SEO effect device, which enables the achievement of all the features required in an optical switch, is that this device is not only bistable in the optical power itself, but is also bistable in the ratio of the input and output optical powers. Hence one can encode a logical “0” (“1”) by a low (high) ratio of the optical beams incident on or coming out of the two SEO effect devices. In fact, the device can be made bistable over a large range of optical powers just by changing the optical power incident on diode 2 [Fig. 3(d)], indicating that the device is capable of showing a new type of gain, known as time-sequential gain [3]. In a device exhibiting time-sequential gain, its transmission can be set by a low-power beam (the control beam). Then the control beam is turned off while a signal beam is incident on the device. Although this signal beam can be of high power, its transmission is controlled by the state of the device, which was set by the low-power control beam. Thus a low-power signal can control a high-power signal, exhibiting a gain that is sufficient to realize a high fan-out. We note that this gain does not require a critical biasing, as needed in other optically bistable devices. As explained above, the signal and control beams are present at different points of time, thus isolating the input from the output. Since the device is bistable with respect to the ratio of the optical powers, fluctuation of the input power does not degrade device performance as long as the light on both diodes is drawn from the same source. The logic level is again defined by the ratio between the two beams entering or exiting the two diodes; thus both are equally affected by the propagation loss. Hence the logic level is independent of the loss. We note that the value for logic 1 is lower when the optical power is in the nanowatt range [Fig. 3(d)], leading to reduced contrast between the two logic levels. At lower power, this contrast diminishes further, ultimately making the device unusable. This happens because, at low optical power, the generated photocurrent in the two diodes is small, leading to an equal voltage drop across the two diodes, as explained earlier.

Finally, we analyze the energy consumption and speed of the SEO bistable device. The energy consumption of the device is given by the energy required to charge and discharge the depletion capacitance of the p-i-n diode. Note that successful operation of the SEO device requires efficient light absorption. In practice, absorbing material is embedded in the ring, and the absorption strength of this region is specified in dB/ $\mu$ m. We find that at a wavelength of 1.5  $\mu$ m, for a ring of radius 3  $\mu$ m and an absorptive loss of  $\sim 0.05$  dB/ $\mu$ m, the absorptive loss rate becomes  $\gamma_l/2\pi = 12$  GHz, and the transmission  $t = 0.9$  for critical coupling. Such performance can be achieved with state-of-the-art ring cavities and graphene-based waveguides [20,21]. For a ring resonator with radius  $r$ , thickness  $d$ , and a depletion layer width of  $w$ , the capacitance  $C_d$  is given by  $C_d = 2\epsilon_o\epsilon_d\pi r d/w$ , and so the switching energy is  $E_{switch} = (1/2)C_d V_o^2$ . With a ring radius of 3  $\mu$ m, a ring slab thickness of 400 nm, a depletion layer width of 1  $\mu$ m, and an applied voltage of 4 V (as derived from the simulations), we find the switching energy to be  $\sim 5$  fJ. The electronic speed of operation will be limited by the speed of the feedback loop. For a resistance of  $\sim 1.5$  k $\Omega$ , the electronics-limited speed of operation is

$\sim 100$  GHz. However, the operational speed will also be limited by the photonic cavity quality factor to  $(\gamma_c + \gamma_l)/\pi \sim 24$  GHz.

We have analyzed the performance of a cavity-assisted SEO bistable device in a silicon photonics platform. The device can be made bistable at very low optical power, as the bistability is not caused explicitly by (comparatively weak) nonlinear effects. This is due to positive optoelectronic feedback created by connecting an electro-optic modulator and a detector. The switching energy of the device can be quite low ( $\sim 5$  fJ) while maintaining a speed of  $\sim 20$  GHz.

A. M. acknowledges useful discussion with Feng Wang, Jelena Vuckovic, and David Miller.

## References

1. H. Gibbs, *Optical Bistability Controlling Light With Light* (Academic, 1985).
2. D. A. B. Miller, *Nat. Photonics* **4**, 3 (2010).
3. A. L. Lentine and D. A. B. Miller, *IEEE J. Quantum Electron.* **29**, 655 (1993).
4. M. Hochberg and T. Baehr-Jones, *Nat. Photonics* **4**, 492 (2010).
5. Y.-H. Kuo, Y. K. Lee, Y. Ge, S. Ren, J. E. Roth, T. I. Kamins, D. A. B. Miller, and J. S. Harris, *Nature* **437**, 1334 (2005).
6. J. K. Doylend, P. E. Jessop, and A. P. Knights, *Opt. Express* **18**, 14671 (2010).
7. X. Gan, R.-J. Shiue, Y. Gao, I. Meric, T. F. Heinz, K. Shepard, J. Hone, S. Assefa, and D. Englund, *Nat. Photonics* **7**, 883 (2013).
8. Y. Tang, H.-W. Chen, S. Jain, J. D. Peters, U. Westergren, and J. E. Bowers, *Opt. Express* **19**, 5811 (2011).
9. A. Yariv, *IEEE Photon. Technol. Lett.* **14**, 483 (2002).
10. Q. Xu and M. Lipson, *Opt. Lett.* **31**, 341 (2006).
11. M. Notomi, A. Shinya, S. Mitsugi, G. Kira, E. Kuramochi, and T. Tanabe, *Opt. Express* **13**, 2678 (2005).
12. K. Nozaki, T. Tanabe, A. Shinya, S. Matsuo, T. Sato, H. Taniyama, and M. Notomi, *Nat. Photonics* **4**, 477 (2010).
13. K. Nozaki, A. Shinya, S. Matsuo, Y. Suzaki, T. Segawa, T. Sato, Y. Kawaguchi, R. Takahashi, and M. Notomi, *Nat. Photonics* **6**, 248 (2012).
14. J.-H. Li, *Phys. Rev. B* **75**, 155329 (2007).
15. G. T. Reed, G. Mashanovich, F. Y. Gardes, and D. J. Thomson, *Nat. Photonics* **4**, 518 (2010).
16. L. Guoliang, A. V. Krishnamoorthy, I. Shubin, Y. Jin, L. Ying, H. Thacker, Z. Xuezhe, K. Raj, and J. E. Cunningham, *IEEE J. Sel. Top. Quantum Electron.* **19**, 95 (2013).
17. C.-H. Liu, Y.-C. Chang, T. B. Norris, and Z. Zhong, *Nat. Nanotechnol.* **9**, 273 (2014).
18. G. Li, X. Zheng, J. Yao, H. Thacker, I. Shubin, Y. Luo, K. Raj, J. E. Cunningham, and A. V. Krishnamoorthy, *Opt. Express* **19**, 20435 (2011).
19. K. Padmaraju, D. F. Logan, X. Zhu, J. J. Ackert, A. P. Knights, and K. Bergman, *Opt. Express* **21**, 14342 (2013).
20. M. Liu, X. Yin, E. Ulin-Avila, B. Geng, T. Zentgraf, L. Ju, F. Wang, and X. Zhang, *Nature* **474**, 64 (2011).
21. Q. Xu, D. Fattal, and R. G. Beausoleil, *Opt. Express* **16**, 4309 (2008).